7 General Concepts on Radioguided Sentinel Lymph Node Biopsy: Preoperative Imaging, Intraoperative Gamma Probe Guidance, Intraoperative Imaging, Multimodality Imaging

Federica Orsini, Federica Guidoccio, Sergi Vidal-Sicart, Renato A. Valdés Olmos, and Giuliano Mariani

Contents

7.1 **Introduction** 151
7.2 **Preoperative Imaging** 153
7.3 **Intraoperative Gamma Probe Guidance** 157
7.4 **Intraoperative and Multimodality Imaging** 159
References 167

Learning Objectives

- To acquire basic knowledge about the role of nuclear medicine imaging in the sentinel lymph node (SLN)
- To understand the SLN concept
- To learn the different steps of sentinel lymph node biopsy (SLNB) consisting of preoperative and intraoperative imaging
- To become familiar with the practical aspects of SLN mapping
- To understand the nuclear medicine issues involved in the mini-invasive surgical approach
- To become familiar with the main steps of intraoperative gamma camera imaging with real-time scintigraphic imaging of the surgical field

7.1 Introduction

SLNB is a diagnostic staging procedure which is routinely employed in the current clinical practice for decision-making in a variety of solid tumor types, above all breast cancer [1] and melanoma [2], in order to assess the tumoral involvement of lymph nodes not only for staging (parameter N of the TNM system) and prognostic stratification, but also for therapeutic purposes [3]. This procedure is part of the so-called radioguided surgery, a whole spectrum of nuclear medicine applications based on the combination of preoperative imaging, intraoperative detection, and postoperative techniques, involving close collaboration between at least three different specialties (nuclear medicine, surgery, pathology, and sometimes radiology and health physics as well) that have rapidly expanded over the last decades [4].

Originally introduced in the early 1990s, the SLN procedure optimizes the detection of occult lymph node metastases in patients without clinical evidence of locoregional involvement. Histopathology of the SLNs so identified and

F. Orsini (✉)
Nuclear Medicine Unit, "Maggiore della Carità" University Hospital, Novara, Italy
e-mail: federica.orsini@maggioreosp.novara.it

F. Guidoccio · G. Mariani
Regional Center of Nuclear Medicine, Department of Translational Research and Advanced Technologies in Medicine and Surgery, University of Pisa, Pisa, Italy

S. Vidal-Sicart
Nuclear Medicine Department, Hospital Clinic Barcelona, Barcelona, Catalonia, Spain

Institut d'Investigacions Biomèdiques August Pi Sunyer (IDIBAPS), Barcelona, Catalonia, Spain

R. A. Valdés Olmos
Department of Radiology, Section of Nuclear Medicine and Interventional Molecular Imaging Laboratory, Leiden University Medical Center, Leiden, The Netherlands

G. Mariani et al. (eds.), *Atlas of Lymphoscintigraphy and Sentinel Node Mapping*,
https://doi.org/10.1007/978-3-030-45296-4_7

resected can distinguish macrometastases (>2 mm in size), micrometastases (between 0.2 and 2 mm), isolated tumor cells (malignant cell clusters <0.2 mm), or positive molecular analysis findings as specified in the eighth edition of the AJCC cancer staging manual [5]. This is possible because attention of the pathologist can now focus on much fewer lymph nodes than those normally retrieved during complete lymph node dissection of a given lymphatic station as customarily done with conventional surgery, so that a more detailed histopathologic examination of the SLNs can be carried out, using more histologic sections (to encompass virtually the entire lymph node) and more sensitive techniques (immunohistochemistry in addition to hematoxylin and eosin staining, and even molecular analysis) [5].

Radioguided surgical procedures are generally less invasive and/or less aggressive than traditional surgical approaches. In the case of radioguided SLNB, instead of a total lymphadenectomy de novo (for example of the homolateral axilla in breast cancer), patients undergo surgical removal of only one (or a few) lymph node(s), thus reducing both immediate and long-term postsurgical complications, such as lymphedema, motor/sensory nerve damage, and functional impairment of the shoulder/arm. This novel surgical strategy is based on the hypothesis that lymphatic drainage to a regional lymph node basin follows an orderly, predictable pattern, and on the function of lymph nodes on a direct drainage pathway as effective filters for tumor cells. This leads us to consider as SLNs all lymph nodes with direct drainage from the primary tumor.

The presence or absence of metastasis in the SLNs has a significant impact on therapeutic strategy. In fact, in patients with early cancer, if the SLN does not contain metastasis, the surgical approach should aim at removing the primary tumor avoiding unnecessary regional node dissection. The likelihood that non-SLNs contain metastasis when the SLN is free from tumor cells is extremely low, thus making extensive lymph node dissection unnecessary in this circumstance. Instead, patients whose SLN contains metastasis usually require dissection of regional lymph nodes. However there is increasing evidence that lymph node dissection can be avoided when the tumor burden in the SLNs is minimal or moderate, such as in particular conditions of early breast cancer [3]. These patients can be managed with different therapeutic strategies, without differences in terms of prognosis than patients treated with axillary dissection. In any case, the SLN status remains a crucial step for the choice of the most appropriate therapeutic strategy [6].

Imaging is made possible by tumoral or peritumoral interstitial administration of a radiopharmaceutical that drains from the injection site through the lymphatic system, and then selectively accumulates by phagocytosis into the macrophages of the SLNs, with consequent prolonged retention. Colloid particles labeled with ^{99m}Tc are currently used for this purpose. The general term "colloid" indicates a class of macromolecules of micellar size varying in size between about 5 and 1000 nm (0.005–1 μm), with similar physicochemical and biological patterns. The speed of lymphatic drainage from the site of interstitial injection and the amount retained in the SLN depend mainly on the size of the radiocolloids, which may be either an inorganic substance (^{198}Au-colloid, ^{99m}Tc-antimony sulfur, ^{99m}Tc-sulfur colloid, ^{99m}Tc-stannous fluoride, ^{99m}Tc-rhenium sulfur) or derived from biological substances (^{99m}Tc-labeled nano- or micro-colloidal human serum albumin). Small-size radiocolloids (smaller than about 100 nm) migrate quite fast from the injection site through the lymphatic system, but they are not efficiently retained in the SLN. On the other hand, larger size radiocolloids are retained more efficiently in the SLN, but their migration from the interstitial administration site is slower.

^{99m}Tc-albumin nanocolloid (that has a quite narrow range of particle size, with over 90% of the particles being smaller than 80 nm) is commercially available and most widely employed in Europe, while ^{99m}Tc-sulfur colloid (with a wide range of particle size between about 20 and 400 nm) is widely employed in the USA.

A novel non-colloidal tracer has recently been introduced in the clinical practice, ^{99m}Tc-tilmanocept. This receptor-targeted radiopharmaceutical consists of a small-sized macromolecule (average diameter 7 nm) of a dextran backbone with multiple units of DTPA (for labeling with ^{99m}Tc) and mannose residues, each covalently attached to the dextran backbone. The uptake mechanism of this radiopharmaceutical in lymph nodes does not depend on the particle size but on avid binding to the CD206 receptors for mannose expressed on the surface of macrophages and dendritic cells in lymph nodes [7].

The advantages of this novel radiopharmaceutical include rapid clearance from the injection site, high SLN extraction, and high SLN retention, with consequent low migration to second-echelon lymph nodes [7, 8].

More recently the hybrid radioactive and fluorescent tracer ICG-^{99m}Tc-nanocolloid has been extensively validated in various malignancies [9]. This bimodal tracer enables preoperative lymphatic mapping thanks to its radioactive component adding intraoperative high resolution based on its fluorescence component. Due to a similar distribution in comparison with ^{99m}Tc-nanocolloid both time schedule and imaging protocol with the hybrid tracer remain unchanged [10].

Lymphoscintigraphy, a mandatory preoperative step of the entire SLNB procedure [11], is normally performed with conventional gamma cameras. When the gamma camera is combined with a CT component to constitute a hybrid SPECT/CT tomograph, the fused images so obtained are highly useful [12], especially in case of complex anatomical

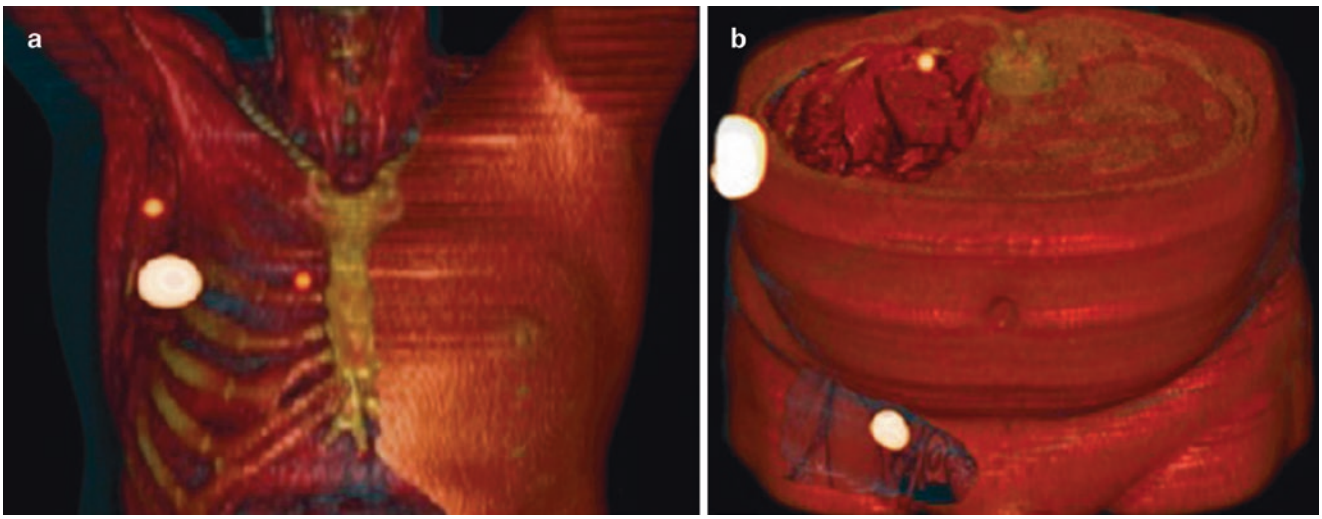

Fig. 7.1 Example of post-processing elaboration of SPECT/CT images. In both cases layers of the tegument have been focally "removed/canceled" asymmetrically between the two sides of the body so as to show the underlying anatomy. (**a**) Lymphoscintigraphy for SLN mapping in a patient with breast cancer, clearly showing migration of ^{99m}Tc-nanocolloid both to an axillary SLNs and to an internal mammary chain SLN. (**b**) Lymphoscintigraphy for SLN mapping in a patient with melanoma at the right flank, clearly showing migration of ^{99m}Tc-nanocolloid both to SLN in the right groin and to a SLN in the retroperitoneal area of the abdomen

regions and/or in case of unusual lymphatic drainage patterns (Fig. 7.1). In fact, hybrid images provide to the surgeon a morphologic and functional roadmap (CT component and SPECT component, respectively) for planning the SLNB procedure with minimal surgical access and operating time.

For immediate decision-making during surgery, intraoperative exploration of the surgical field is performed with the widely validated procedure based on the so-called handheld gamma probe. While this instrumentation produces a numerical readout and an acoustic signal proportional to radioactivity accumulation as a guide in the surgical field, the recently developed portable gamma cameras enable real-time scintigraphic imaging of the surgical field. All these instrumentations allow selective identification of the SLNs to be removed by the surgeon and analyzed by the pathologist. This interaction between technologies and medical disciplines permits to continuously refine the methodology and to improve the outcomes of radioguided surgery.

Key Learning Points

- SLNB is a diagnostic staging procedure that is applied in a variety of tumor types with the aim to determine the tumor status of the SLNs.
- Histopathology of the SLNs so identified and resected can distinguish macrometastases (>2 mm in size), micrometastases (between 0.2 and 2 mm), isolated tumor cells (malignant cell clusters <0.2 mm), or positive molecular analysis findings.
- The interactions between different medical disciplines permit to improve the outcomes of radioguided surgery during SLNB.
- Radioguided surgical procedures are generally less invasive and/or less aggressive than traditional surgical approaches.
- The presence or absence of metastasis in the SLN has a significant impact on therapeutic strategy.
- Imaging is made possible by tumoral or peritumoral interstitial administration of a radiopharmaceutical that drains from the injection site through the lymphatic system, and then selectively accumulates by phagocytosis into the macrophages of the SLNs.
- The radiopharmaceuticals most frequently employed for SLNB are ^{99m}Tc-sulfur colloid, ^{99m}Tc-albumin nanocolloid, and ^{99m}Tc-tilmanocept.

7.2 Preoperative Imaging

Lymphoscintigraphy is generally performed in the afternoon of the day preceding surgery if the operation is scheduled in the early morning, or on the same day 4–6 h prior to surgery, depending on logistics of the institution. For same-day pro-

cedures, a smaller activity of radiocolloid is generally administered (at least 15–20 MBq) compared to the two-day procedure (at least 37–74 MBq).

The gamma camera energy selection peak is centered on the 140 keV of ^{99m}Tc (with ±10% window), and the use of high-resolution collimator(s) and of a 256 × 256 acquisition matrix is preferred; a pinhole collimator may occasionally be used to improve spatial resolution.

While dynamic acquisition is needed especially when a fast lymphatic drainage is expected (head and neck, melanoma, penile, testis, or vulvar cancers), it can nevertheless provide relevant information for identifying the actual SLNs (versus higher echelon nodes) also in the case of other malignancies, particularly breast cancer. Concerning in particular breast cancer, the patient is positioned supine with her arms raised above the head, and the collimator is placed as close as possible to the axillary region. Anterior, anterior-oblique, and lateral images are acquired. A ^{57}Co flood source can be positioned beneath the patient's body in order to obtain some reference anatomic landmarks in the scintigraphic image (Figs. 7.2 and 7.3). Alternatively, the body contour can be identified by moving a ^{57}Co or ^{99m}Tc point source along the patient's body during scintigraphic acquisition (Fig. 7.4).

Besides SLN identification, lymphoscintigraphy is also useful to identify other possible unusual paths of lymphatic draining, such as the internal mammary chain or even intramammary, interpectoral, or infraclavicular lymph nodes in case of breast cancer [11] (Fig. 7.5), or in case of additional SLNs in areas of deep lymphatic drainage such as the pelvis, abdomen, or mediastinum. Especially in these cases, SPECT/CT imaging is important since it directly demonstrates anatomical localization of SLNs and obviates the problem of identifying anatomic landmarks as a reference for topographic intraoperative location of the SLNs [12–14]. Moreover, SPECT/CT imaging is highly recommended to localize SLNs in areas with complex anatomy and a high number of lymph nodes (such as the head and neck) and/or in case of absent visualization of SLN at planar imaging. In this occurrence, it is only SPECT/CT imaging that can allow SLN identification; in fact, due to the correction for tissue attenuation SPECT/CT imaging is more sensitive than planar imaging and is generally particularly useful in obese patients (Fig. 7.6).

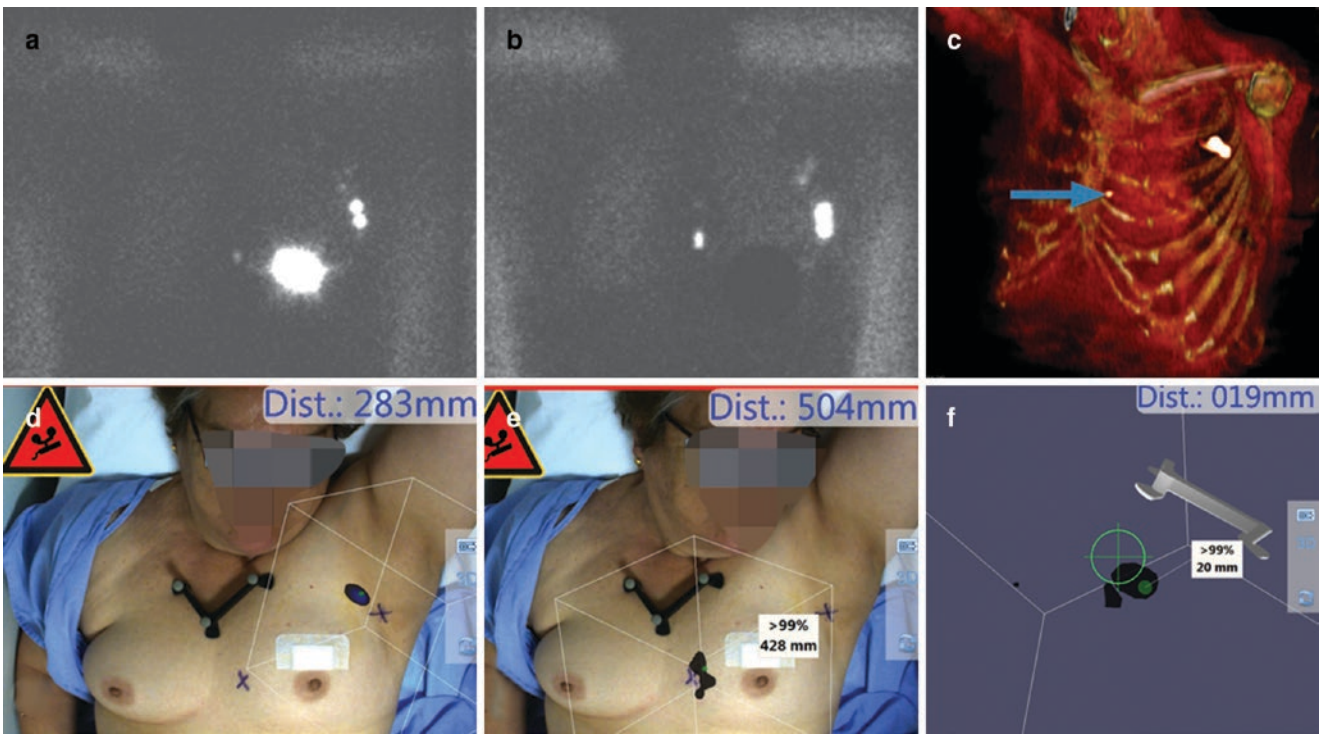

Fig. 7.2 Upper panels: planar scintigraphy (with flood phantom for body contour, see further below) obtained in a breast cancer patient about 30 min after injecting ^{99m}Tc-nanocolloidal albumin intratumorally (**a**). Besides intense radioactivity remaining at the injection site, left image shows migration of the radiocolloid to axillary SLNs and to the internal mammary chain area. Central image (**b**) was taken 2 h later, using a lead plate to cover the injection site. Axillary hot spots are clearly depicted, as well as the hot spot in left parasternal area. Right image (**c**) shows a 3D volume rendering displaying the SLNs: two in left axilla and one (arrow) in the third left intercostal space. Lower panels show overlay of the freehand SPECT 3D image on the intraoperative video image of the same patient, for easier anatomical correlation. Panel (**d**) shows the axilla with visualization of lymph nodes. Panel (**e**) shows the display of internal mammary node. Panel (**f**) shows intraoperative visualization of the SLN in the left axilla when gamma probe is 19 mm away

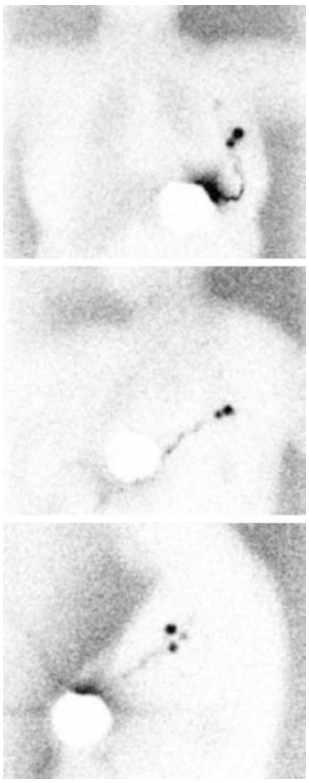

Fig. 7.3 Planar lymphoscintigraphy of breast cancer patient obtained between 20 and 30 min after injecting about 111 MBq of ^{99m}Tc-nanocolloidal albumin peri-areolarly in a patient with cancer of left breast. Upper row shows anterior projection, central row depicts oblique view, and lower row shows lateral projection. Images were taken using a lead circle to cover the injection site. All images were acquired using a single-head gamma camera and a high-resolution, low-energy collimator (acquisition time 2 min). The ^{99m}Tc flood phantom placed opposite to the gamma camera head produces the body contour delineation. While two axillary SLNs are visualized in the anterior and oblique projection, three nodes are visualized in the lateral projection

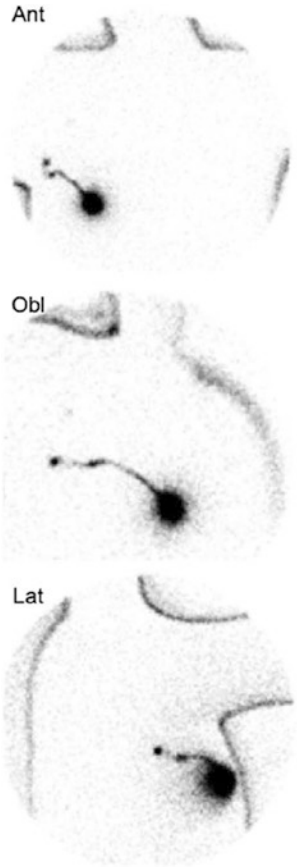

Fig. 7.4 Body contour delineation obtained by moving a ^{57}Co point source along the body of the patient during acquisition of the planar scintigraphic images. In this patient with cancer of the right breast, ^{99m}Tc-nanocolloidal albumin was injected peri-areolarly. Images acquired in the anterior projection (upper panel), right anterior oblique projection (central panel), and right lateral view (lower panel) visualize migration of the radiocolloid through a lymphatic channel to a single SLN in the axilla

However, SPECT/CT imaging does not replace planar lymphoscintigraphy, but it must rather be considered as a complementary imaging modality. In fact, contrary to SPECT/CT, planar lymphoscintigraphy allows to mark the cutaneous projection of the SLN with a dermographic pen, in order to help the surgeon to localize the site for the best surgical access. In current protocols SPECT/CT imaging is performed following delayed planar imaging (mostly 2–4 h after radiocolloid administration). This sequence of acquisitions is helpful to clarify the role of both modalities. Sequential planar acquisitions allow better visualization of the routes of lymphatic drainage. Dynamic planar acquisition usually consists of sets of serial frames (generally 1–5 min each) or sequential sets of static images in the preset count mode (generally 300,000–500,000 counts) acquired starting immediately after radiocolloid injection and up to clear scintigraphic visualization of the lymphatic routes and SLNs.

Multiplanar reconstruction enables two-dimensional display of fusion images in relation to CT and SPECT, and the use of cross-reference lines allowing the navigation between axial, coronal, and sagittal views. At the same time this tool leads to correlate radioactive SLNs seen on fused SPECT/CT with lymph nodes seen on CT (Fig. 7.7a, b). This information is helpful during the intraoperative procedure, as well as to assess completeness of excision—using portable gamma cameras or probes.

Fused SPECT/CT images can also be displayed using maximum intensity projection reconstruction. This tool enables three-dimensional display, and improves anatomical localization of SLNs (Fig. 7.7c).

When using volume rendering for three-dimensional display, different colors are assigned to anatomical structures such as muscle, bone, and skin. This leads to identifying of better anatomical reference points and incorporating of an additional dimension in the recognition of SLNs (Fig. 7.7d).

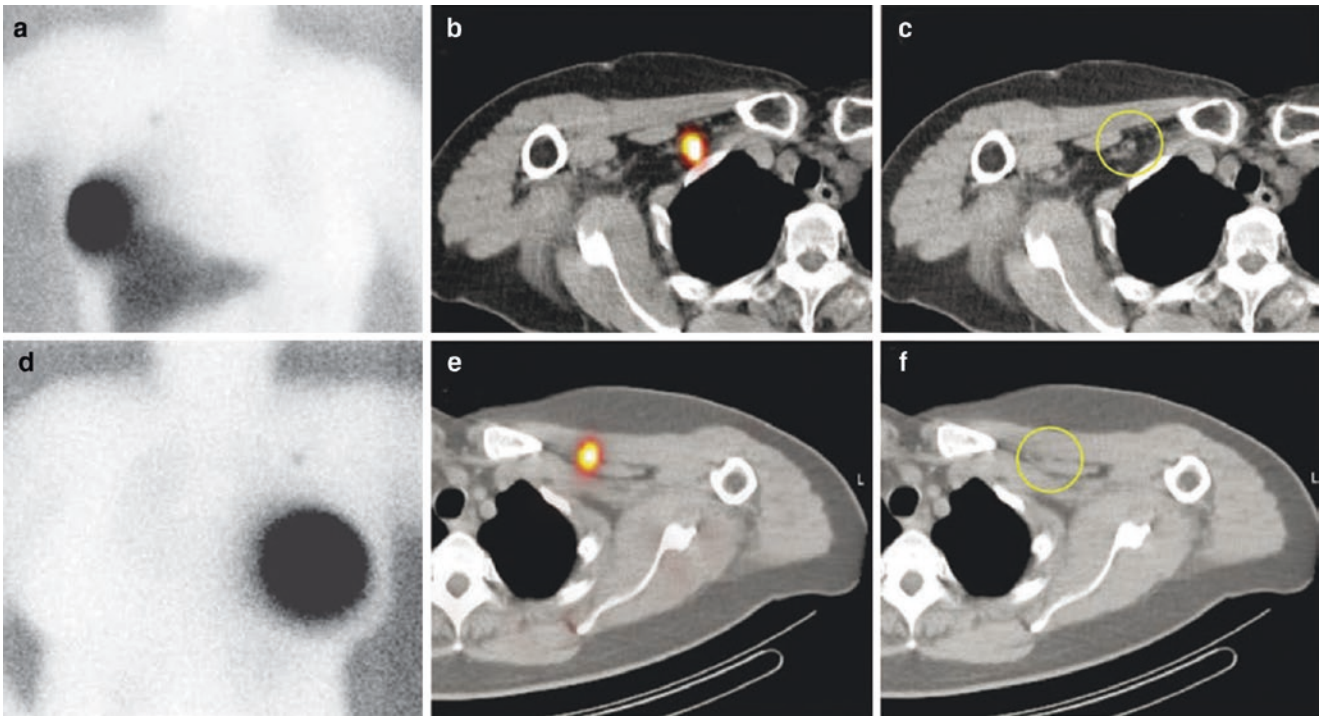

Fig. 7.5 Added value of SPECT/CT imaging in two different patients in whom planar scintigraphy shows focal uptake in the retroclavicular area; the patients had cancer located in the right breast (**a**) and in the left breast (**d**), respectively. Fused axial SPECT/CT sections (**b** and **e**), showing the location of the two SLNs between the pectoral muscles. These SLNs correspond to two single lymph nodes in the CT images (**c** and **f**, yellow circle), respectively

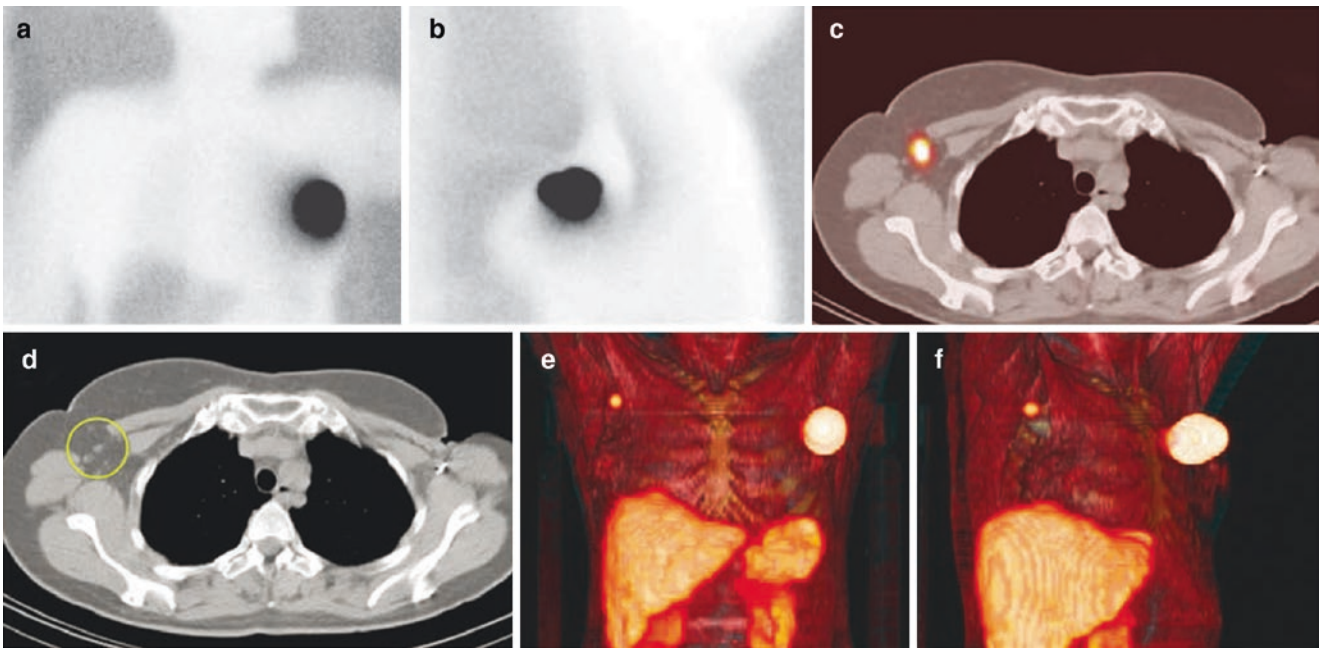

Fig. 7.6 Example of lymphatic drainage to the contralateral axilla in a patient with breast cancer. Anterior (**a**) and left lateral (**b**) planar images showing no drainage from the site of intratumoral radiocolloid injection in the left breast (body contour obtained with a flood source placed beneath the patient's body). By contrast, on the fused axial SPECT/CT image a SLN is clearly visualized at the border of the right pectoral muscle (**c**), corresponding to a single lymph node on the CT image (**d**, yellow circle). This SLN is displayed using 3D volume rendering for a better anatomical recognition in the anterior (**e**) and in the right anterior-oblique views (**f**)

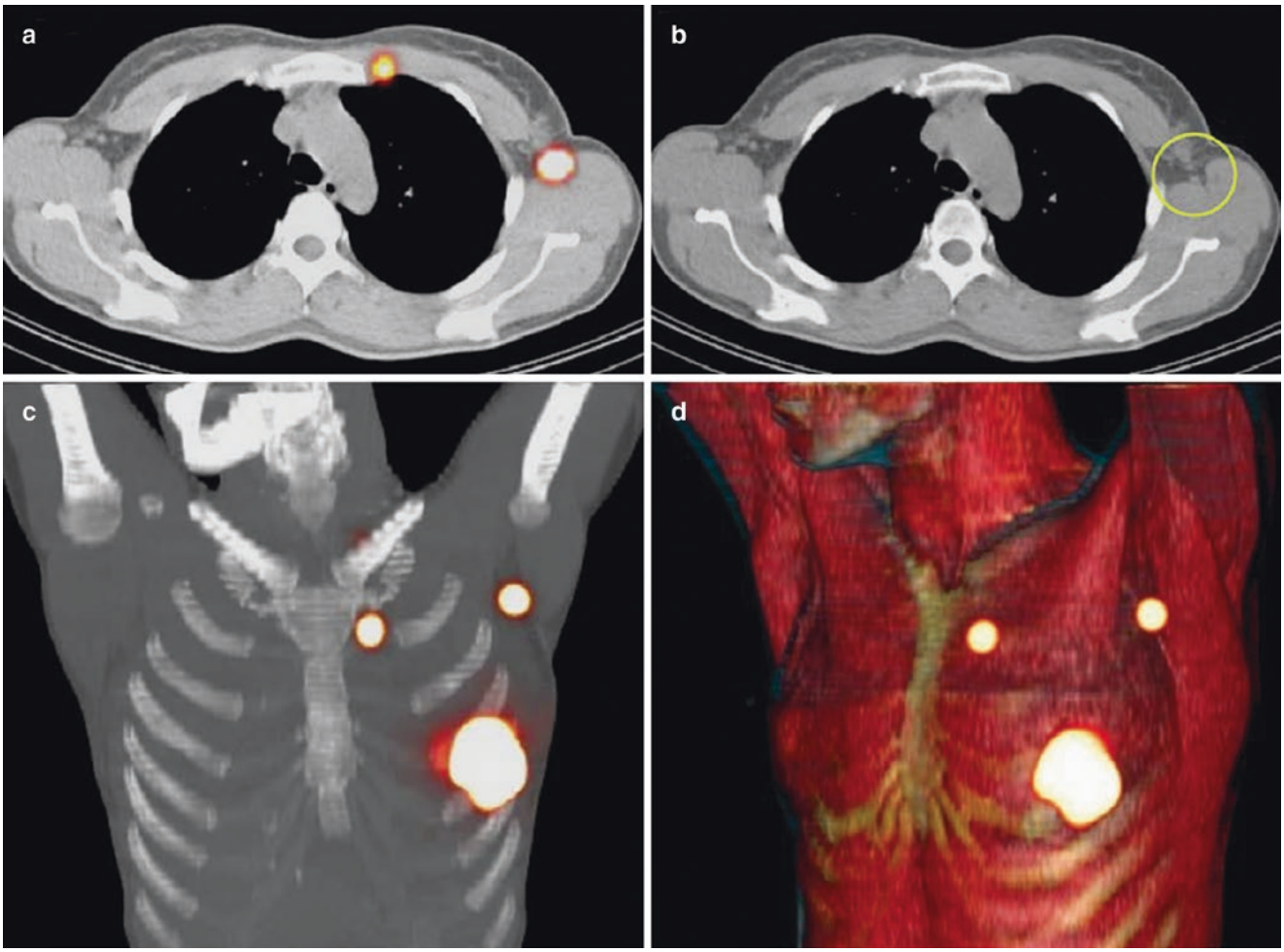

Fig. 7.7 (**a**) Fused axial SPECT/CT section obtained during lymphoscintigraphy in a patient with breast cancer, showing two SLNs, respectively, in the left internal mammary chain and in the left axilla; the yellow circle in (**b**) corresponds to a small lymph node seen on axial CT. (**c**) Fused coronal SPECT/CT displayed as maximum intensity projection (MIP), showing a SLN in the left axilla and an internal mammary chain SLN in the second left intercostal space. (**d**) SPECT/CT with volume rendering for 3D display, showing the two SLNs, respectively, in the left internal mammary chain and in the left axilla with their anatomic localizations with reference to muscles and bones

Key Learning Points

- Lymphoscintigraphy is a mandatory preoperative step of the SLNB procedure and it is normally performed with conventional gamma cameras.
- Added SPECT/CT images improve SLN detection by providing anatomical landmarks, especially regions with complex and/or unusual lymphatic drainage patterns.

7.3 Intraoperative Gamma Probe Guidance

The gamma probe is used to count radioactivity in the surgical field intraoperatively, without producing any scintigraphic image but yielding both a numerical readout and an audible signal, which is proportional to the counting rate.

The detector is usually of limited size, basically a long narrow cylinder with diameter of 10–18 mm, sometimes slightly angled in order to allow easier handling within the surgical field. The gamma probe can be utilized in the

surgical field because it is made of a material that can be sterilized (usually metal), or it can simply be covered with a sterilized wrapping (such as those used for intraoperative ultrasound probes). Through the digital readout and acoustic signal, the gamma probe enables the surgeon to precisely localize areas of maximum radioactivity accumulation, thus guiding identification and removal of the target tissue [15, 16].

The commercially available gamma probes can be divided into crystal scintillation and semiconductor probes. Further technical features of the probe vary depending upon whether the radiopharmaceuticals are labeled with ^{99m}Tc or other radionuclides, including positron-emitting radiopharmaceuticals [17–19].

The probe is connected to a small control unit, equipped with a portable laptop or tablet, usually with a flexible cable that may also be covered with sterilized wrapping; Bluetooth-based connections have now become available, permitting easier use of the entire instrument in the operating room. Energy window for detection/counting is usually around 140 Kev (for ^{99m}Tc-labeled radiopharmaceuticals), but can vary depending on the radionuclide employed. At the same time the unit usually emits an audible signal, the pitch/tone of which varies proportionally to the counting rates. The acoustic signal helps the surgeon to explore the surgical field without looking at the control unit display.

Sensitivity (counting rate per unit of radioactivity), energy resolution (ability to detect "true" counts arising in the target versus secondary scattered radiation), spatial resolution (ability to identify very close radioactive sources as distinct from each other), and linearity of counting (it relates to the dead time) are the most important parameters of the probe in detecting radiation. Therefore, the main important tasks of a probe include sufficient sensitivity (to identify a weakly active SLN when attenuated by, typically, up to 5 cm of soft tissue), and energy and spatial resolution (to discriminate activity of a certain energy within the SLN from that originating from other sites).

More recently, with the development of PET techniques, intraoperative probes specifically designed to detect the high-energy photons originated by the annihilation process have become commercially available, thus making it possible to use radioguidance also with PET radiopharmaceuticals [20–22].

Nevertheless, major advantages of the whole process of SLN mapping in both the preoperative and the intraoperative phases have been made possible by the use of SPECT/CT and/or intraoperative imaging probes, providing a set of anatomo-topographic information that guides resection through the optimal surgical access according to the principle of least invasive surgery [23, 24]. As exemplified in Fig. 7.8, this approach is especially useful when planning surgery in complex anatomical regions such as the head and neck or the pelvis [25–31].

Just before starting surgery and with the patient already positioned on the operating table, the gamma probe is initially utilized to scan the SLN basin(s) and/or any other region where radiocolloid accumulation has been visualized, in order to confirm correct identification of the SLNs. Using the images and skin markings as guides, the probe (placed over the regions of highest counts) can be used to select the optimum location for incision. After incision, the probe is then introduced through the surgical field to explore the

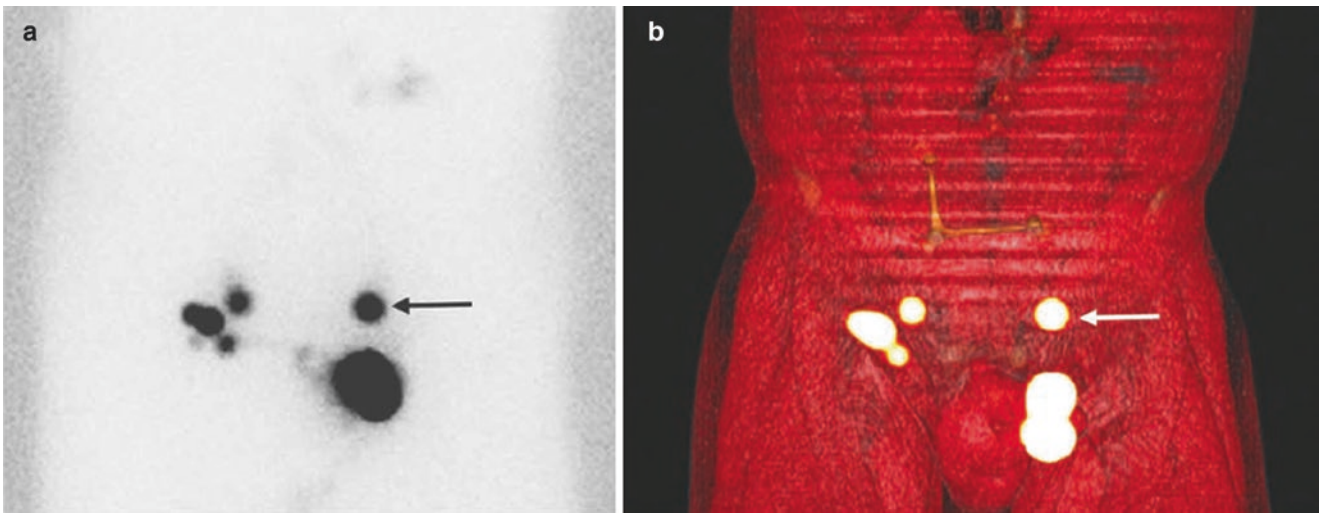

Fig. 7.8 (**a**) Planar anterior image showing lymphatic drainage to both sides, seemingly to groin lymph nodes (single SLN indicated by arrow on the left side) in a patient with penile cancer. (**b**, **c**) SPECT/CT with volume rendering for 3D display, respectively, in the anterior view and in a cranial view (in the latter, the bottom side corresponds to the anterior side of the body). (**d**) Fused axial SPECT/CT section showing anatomic localization of three of the lymph nodes (two on the right and one on the left) at different depths in the pelvis

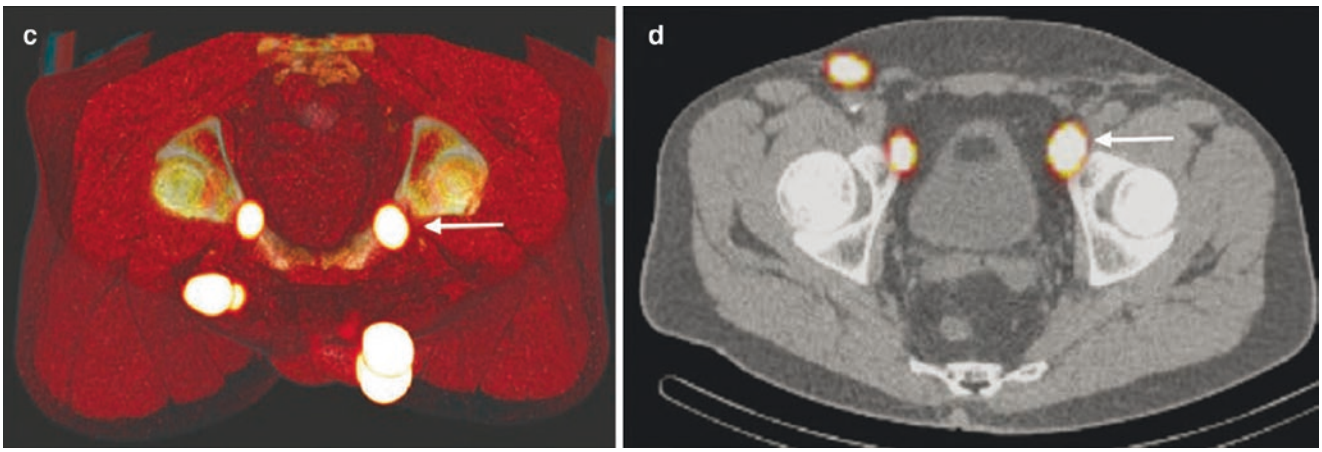

Fig. 7.8 (continued)

expected localization of the SLNs, which are usually easily identified by acoustic signal thanks to high target/background count rates. After removing the radioactive lymph nodes, the operative field is explored again with the gamma probe, assessing any residual radioactivity to confirm removal of the hot node(s). If necessary, the search must continue for possible further radioactive lymph nodes. The SLN and any other nodes so identified are then sent for complete histopathologic analysis.

Counts are recorded per unit time with the probe in the operative field, over the node before excision (in vivo) and after excision (ex vivo). A background tissue count is also recorded with the probe pointing away from the injection site, nodal activity, or other physiologic accumulations (i.e., liver) [32].

In breast cancer, once the learning phase of SLNB has been completed, the success rate of lymphoscintigraphy and intraoperative gamma probe counting in identifying SLNs is higher than 96–97% in experienced centers. This value is greater than that commonly experienced using blue dye alone (75–80%), while combining radioguidance with the blue dye leads to a 98–99% success rate in SLN identification [33]. The blue dye can be injected around the primary tumor or scar (in a similar way as the radiocolloid was injected) 10–20 min prior to the operation. Administration should be performed after the patient is anesthetized, to avoid a painful injection. Within 5–15 min the SLN is colored. Currently, the most commonly used dyes are patent blue V, isosulfan blue, and methylene blue. The additional value of dyes may be observed in cases with macrometastasis in the SLN. In fact, such SLN involvement may inhibit radiocolloid accumulation, if tumor cells have replaced most of the normal lymph node tissue [34]. In these cases a new first draining node is seen (Fig. 7.9) that can result in a false-negative finding [26]. To decrease false-negative results, the open axilla should be palpated and suspicious lymph nodes harvested, even if they are neither hot nor blue. In cases of non-visualization or if the SLN is located outside the lower medial part of the axilla, palpation of the typical SLN area is particularly important [32, 35].

A notable disadvantage of using blue dyes instead of radiotracers is that blue dyes are not helpful when extra-axillary nodes (internal mammary or supraclavicular) are to be evaluated [36, 37].

Key Learning Points

- Intraoperative exploration of the surgical field is performed with the widely validated procedure based on the so-called handheld gamma probe.
- This instrumentation produces a numerical readout and an acoustic signal proportional to radioactivity accumulation, as a guide in the surgical field for SLN detection and localization.

7.4 Intraoperative and Multimodality Imaging

Currently, the trend of surgery is towards adopting minimally invasive approaches for a growing spectrum of procedures. This includes oncological surgery, as it implies much faster postsurgical recovery of patients. For optimally planning and performing these approaches, the most crucial issue is accurate preoperative characterization of the surgical strategy, which is achieved through diagnostic imaging. In this regard, maximum benefit for the success of minimally invasive surgery derives from integration of anatomical (e.g., CT) and metabolic/functional imaging, the latter being typically provided by nuclear medicine procedures. These features contribute to a better characterization of the lesion to be

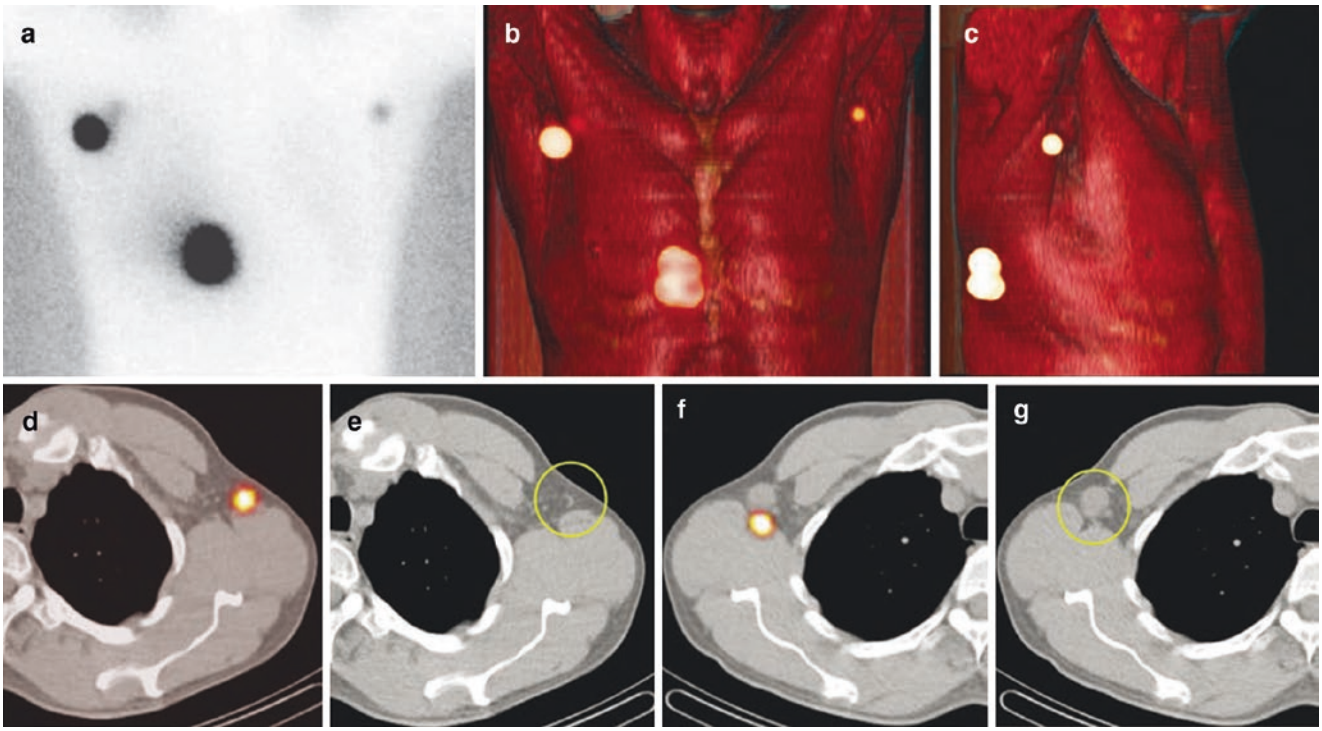

Fig. 7.9 Upper panels: (**a**) planar anterior view acquired in a patient with melanoma located in the back of the right torso, showing lymphatic drainage to both axillae, as better demonstrated by SPECT/CT with volume rendering for 3D display, respectively, in the anterior and in the right oblique view (**b** and **c**). Lower panels: fused axial SPECT/CT section at two different levels, showing the location of radioactive lymph nodes, respectively, in the left axilla (**d**) and in the right axilla (**f**). The corresponding CT sections show that the hot lymph node in the left axilla corresponds to a normal-sized node (yellow circle in panel **e**), while in the right axilla the hot lymph node (of approximately normal size) is located posterior to a grossly enlarged, most likely metastatic lymph node not visualized by lymphoscintigraphy (yellow circle in panel **g**)

removed, and in many cases enable subsequent intraoperative guidance through the use of devices especially designed for this use [38, 39].

Over the last decade, intraoperative imaging probes have become commercially available for clinical practice, and the use of such handheld portable gamma cameras is increasing. By providing real-time imaging with a global overview of all radioactive hot spots in the whole surgical field [40], intraoperative imaging with portable gamma cameras can be used either during open surgery or during laparoscopic procedures; the information so gained can be combined with data obtained with conventional or laparoscopic gamma probe counting [41, 42].

Information provided by these devices can be combined with those ones obtained preoperatively by lymphoscintigraphy or SPECT/CT. Using the anatomic landmarks provided by SPECT/CT images, the portable device can be oriented to surgical targets in the operating room [43]. No delay has to elapse between image acquisition and display (real-time imaging), with the possibility of continuous monitoring and spatial orientation on the screen. Real-time quantification of the count rates recorded should also be displayed.

The development of such cameras is shown in Fig. 7.10. While the earliest devices were heavy handheld devices, the new generation of such equipment includes portable gamma cameras that are lighter, or equipped with stable support systems.

Among the products commercially available, one of the most used devices is equipped with a CsI(Na) scintillation crystal and different collimators (pinhole collimators, 2.5 and 4 mm in diameters, and divergent). The pinhole collimator enables to visualize the whole surgical field (depending on the distance between the camera and the source). The field of view varies between 4 cm × 4 cm at 3 cm from the source and 20 cm × 20 cm at 15 cm from the source. This device has been integrated in a mobile and an ergonomic support that is easily adjustable. The imaging head is located on one arm that allows optimal positioning on the specific area to be explored.

Another approach is based on the use of CdZnTe detectors. For instance, the detector is made of a single tile of CdZnTe, patterned in an array of 16 × 16 pixels at a pitch of 2 mm. The head is equipped with a series of interchangeable parallel-hole collimators to achieve different performances

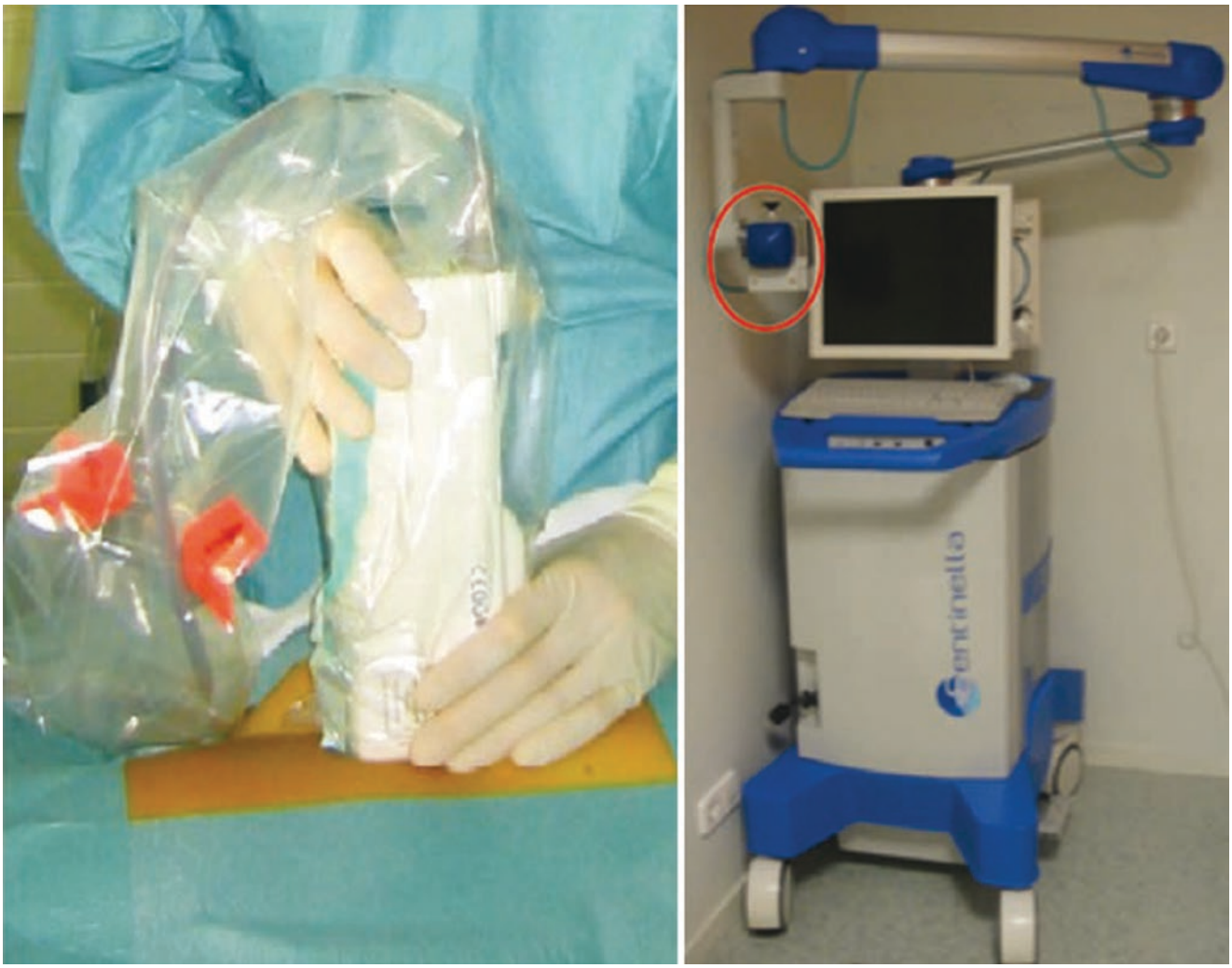

Fig. 7.10 Example of portable gamma cameras. Left panel: lightweight portable gamma camera (less than 1 kg), without support system. Right panel: recent-generation portable gamma camera with improved ergonometry and adequate and stable support system for intraoperative use; this unit incorporates a laser pointer to center the image and adjust the scanning procedure

in terms of spatial resolution and/or sensitivity. The field of view is 3.2 cm × 3.2 cm and the weight is 800 g [44].

A further development is represented by an intraoperative gamma camera that is still based on the CdZnTe pixel technology, and has originally been developed for breast imaging. The field of view is 13 cm × 13 cm and the intrinsic spatial resolution is 2 mm. This camera is also equipped with interchangeable parallel-hole collimators and is integrated in a workstand articulated arm.

However, since non-imaging probes are still the standard equipment for detection of radiolabeled tissue in the operating room, the role of intraoperative imaging is generally limited, at least so far, to constitute an additional aid to the surgeon to identify the SLN. Some authors have assessed the added value of portable gamma camera in clinical practice. The usefulness of the portable gamma cameras in breast cancer patients is being established in the following conditions: (a) when no conventional gamma camera is available, (b) in particular cases with difficult drainage or extra-axillary drainage (intramammary and internal mammary chain nodes) [45], (c) in case of only faint lymph nodal radiocolloid uptake, (d) when the SLN is located very close to the injection site, or (e) in case of significant photon emission and scatter from the injection site. In fact, the position of the portable gamma camera can be moved and adjusted in such a manner so as to acquire special-angle views in order to also show SLNs near the injection area.

The use of an intraoperative imaging device implies the possibility to monitor the lymphatic basin before and after removal of the hot nodes, to verify completeness of lymph node excision [46] (Fig. 7.11). After excision of each lymph node, a new image is acquired and compared

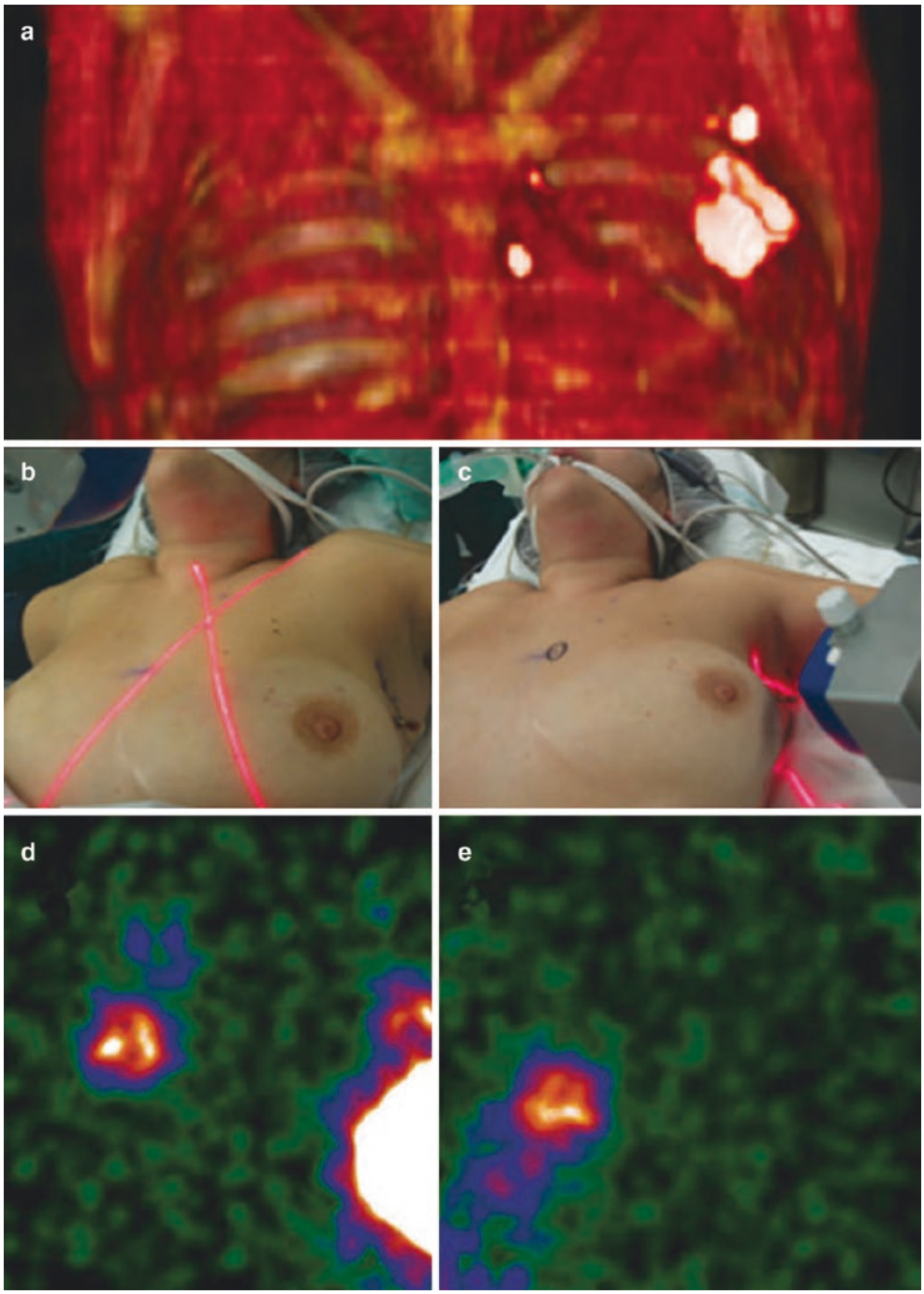

Fig. 7.11 Preoperative images in a 42-year-old patient with a T1 cancer in her left breast. (**a**) 3D reconstruction image after processing SPECT/CT data. (**b**) A scintigraphic anterior view is acquired by placing the portable gamma camera in previously marked points on the skin (inner mammary chain, see laser cross pointers). (**c**) The portable gamma camera can be placed in different positions to better depict the lymph nodes; in this picture it is tilted in an oblique view. (**d**) Visualization of an inner mammary chain lymph node, with partial vision of the injection site (image corresponding to the position of the gamma camera as in panel **b**). (**e**) Visualization of an axillary lymph node depicted with the gamma camera positioned as in panel **c**

with the image acquired before excision (Fig. 7.12). If focal radioactivity remains at the same location, it is concluded that another possible SLN is still in place. Thus, the use of a portable gamma camera in addition to the gamma probe is important to provide certainty on whether all SLNs have been adequately removed (Fig. 7.13) [47].

In the operation room, the gamma camera can be placed above the previously marked SLN locations using some external point sources (like ^{133}Ba, ^{153}Gd, or ^{125}I); alternatively, in some gamma cameras a laser pointer is fitted to the device. In those devices where a laser pointer is included, it is displayed as a red cross over the patient's skin. The position of this red cross is visible on the computer screen of the equipment.

During surgery, an initial 30–60-s image is acquired with the gamma camera to assess the surgical field and validate SLN uptake. This time can be longer when the lymph nodes are depicted as areas with faint focal uptake. After incision, if there is any difficulty in finding the precise location of the

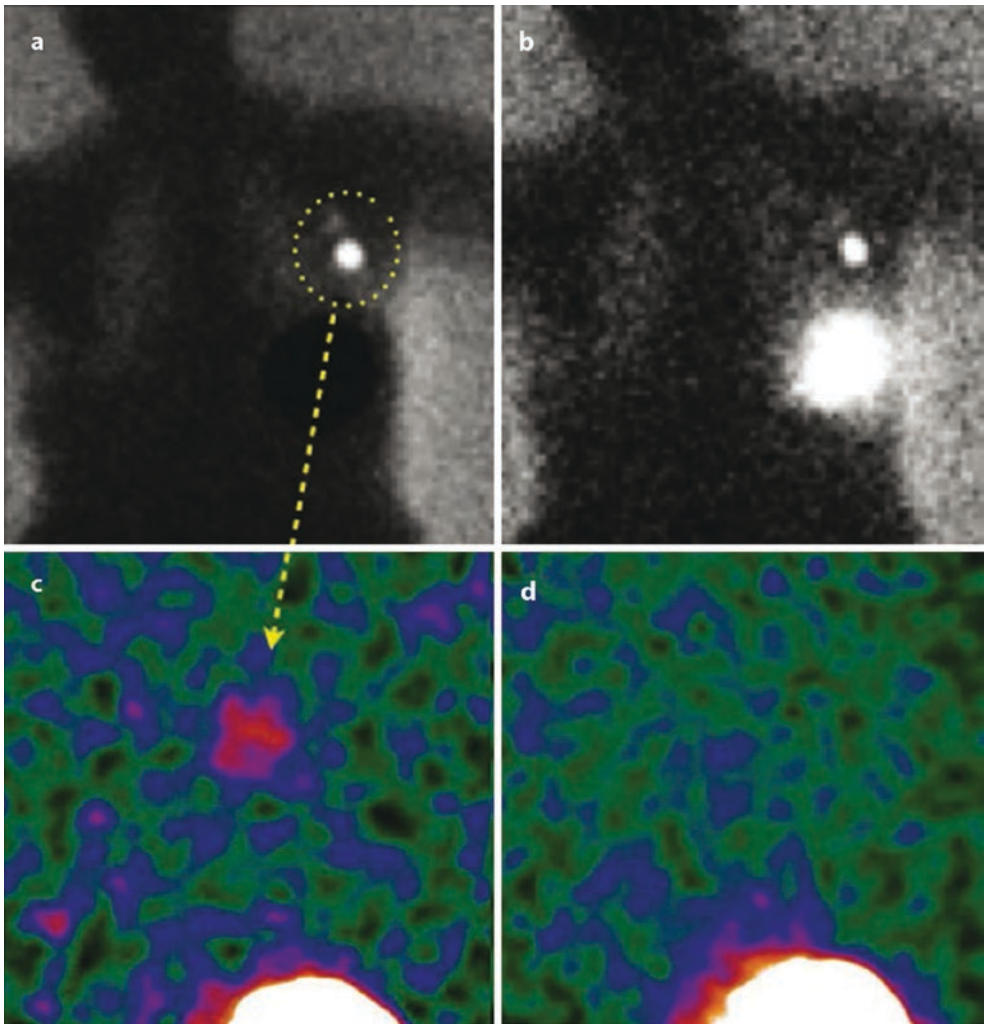

Fig. 7.12 (**a**) Lymphoscintigraphic image acquired with a conventional, large-field-of-view gamma camera 2 h after intratumoral injection of 111 MBq of ^{99m}Tc-nanocoll in a 57-year-old patient with breast cancer in her left upper outer quadrant; at least one axillary SLN is clearly depicted (yellow circle). (**b**) The same image without lead shielding of the injection site shows similar radiocolloid distribution. (**c**) Operating room image obtained with a portable gamma camera prior to starting the SLN procedure, confirming similar findings (yellow arrow). (**d**) Image obtained with the portable gamma camera after completing radioguided SLN excision, showing no residual activity except the intratumoral injection site. The use of the portable gamma camera, in addition to the handheld, non-imaging gamma probe, was especially useful to confirm the completeness of SLN removal

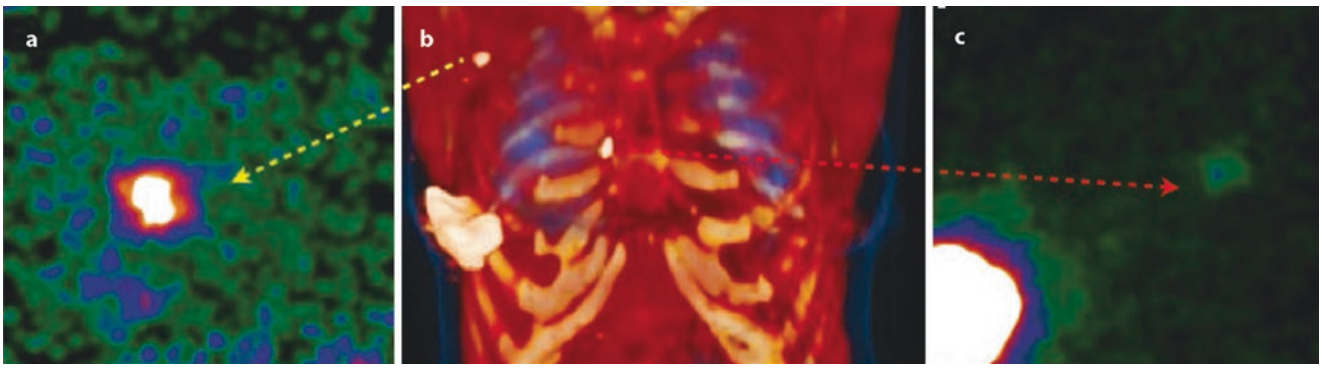

Fig. 7.13 Utility of the portable gamma camera during surgery for the certainty of SLN resection. Radiotracer uptake displayed on gamma camera (**a**), corresponding to the node depicted in the axillary area (yellow arrow) on the 3D volume-rendering reconstruction of a breast cancer patient with lymphatic drainage to axilla and inner mammary chain (**b**). Parasternal SLN (red arrow) is depicted with the gamma camera as well (**c**). Preoperative image of the axilla shows a highly active SLN (**d**). Image after axillary node retrieval informs about the absence of other significant tracer uptake (**e**). Similar approach in the internal mammary chain SLN (**f**, **g**)

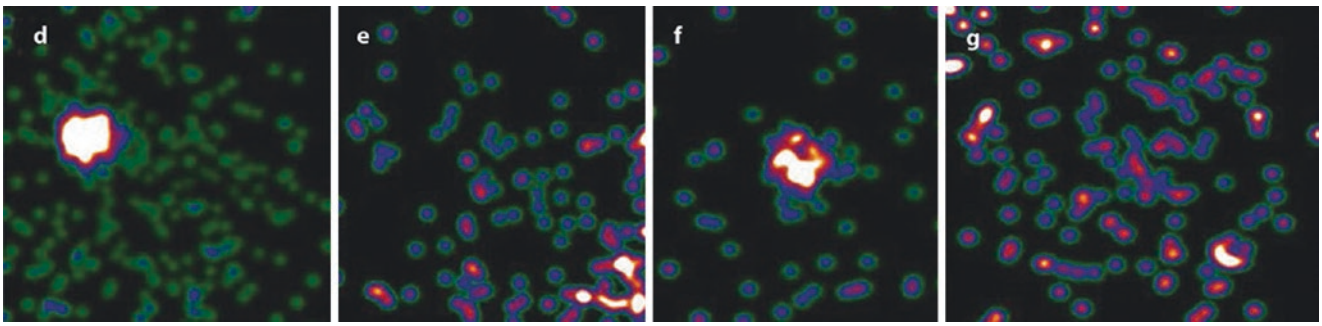

Fig. 7.13 (continued)

SLN using the gamma probe, another 30–120-s image, depending on the level of lymph node uptake, is acquired using the portable gamma camera.

The use of the external point sources facilitates SLN localization, as these sources can be depicted separately on the screen of the portable gamma camera, thus functioning as a pointer in the search for the nodes. The matching of two signals (^{99m}Tc signal and ^{153}Gd, ^{133}Ba, or ^{125}I pointer signals) indicates the correct location of the SLNs. This location is then checked using the gamma probe. After SLN retrieval, another set of images is acquired to ascertain the absence of the previously visualized SLNs, or to ascertain the presence of remaining radioactive nodes (additional SLNs or second-tier nodes, see Fig. 7.14).

Thanks to novel technological possibilities, combining a spatial localization system and two tracking targets to be fixed on a conventional, handheld gamma probe results in new 3D visualization of the traditional acoustic signal of the gamma probe. This feature, together with the real-time information on depth that the system may provide, would expand the applications of radioguided SLNB in oncology, particularly for malignancies with deep lymphatic drainage [48, 49]. In this regard, the most interesting development in radioguided surgery is the so-called system free-hand SPECT, in which a continuous positioning system installed in the operating room is based on a fix pointing device, on the patient's body, and, respectively, on the handheld gamma counting probe, thus permitting a virtual reconstruction in a 3D environment. Position of the gamma probe relative to the fix device is tracked by infrared positioning technology, and the output of the intraoperative gamma probe is spatially co-registered in the surgical field (depicted by a video camera) and displayed on a monitor in which the surgeon can easily check location and depth of the foci of radioactivity accumulation to be resected. This 3D information may be further used for precise localization and targeting of the radioactive SLNs and of tumor tissue, thus implementing a radioguided navigation system. The device can ensure permanent assistance and transparent documentation of soft-tissue removal during the intervention (Figs. 7.15 and 7.16).

On the other hand, the possibility of combining the current radiopharmaceuticals with other agents opens new fields to explore. In this regard, a radiolabeled nanocolloid agent has been combined with ICG, a fluorescent agent, for SLN detection in robot-assisted lymphadenectomy [50].

In contrast to the use of a single-fluorescent agent [51, 52], this bimodal tracer may allow the surgeons to integrate the standard approach based on radioguided detection with a portable gamma camera with a new optical modality based on fluorescent signal detection. This approach is being successfully applied in various malignancies (Fig. 7.17) [53], since the hybrid approach (ICG-^{99m}Tc-nanocolloid) provides the ability to perform radioguidance and enhance it by fluorescence imaging of the exact same features. This results in a further refinement of the surgical SLN identification, e.g., the ability to surgically identify SLNs in close proximity to the injection site. The synergistic approach also yields enhanced intraoperative SLN identification/retrieval rates.

Key Learning Points

- Portable gamma cameras enable real-time scintigraphic imaging of the surgical field and helps in SLN identification and verification of completeness of SLN excision.
- Products commercially available support different technologies such as CsI(Na) scintillating crystal, CdZnTe detectors, and combinations of spatial localization system and tracking targets fixed on a conventional handheld gamma probe, the latter resulting in new 3D visualization of the surgical field.
- During surgery, an initial fast image is acquired with the portable gamma camera to assess the surgical field and validate SLN uptake; after the incision, a second image is acquired to confirm complete resection of radioactive lymph nodes.
- Combining current radiopharmaceuticals with other agents, such as fluorescent agents, opens new fields to explore different compounds for SLN identification and removal.

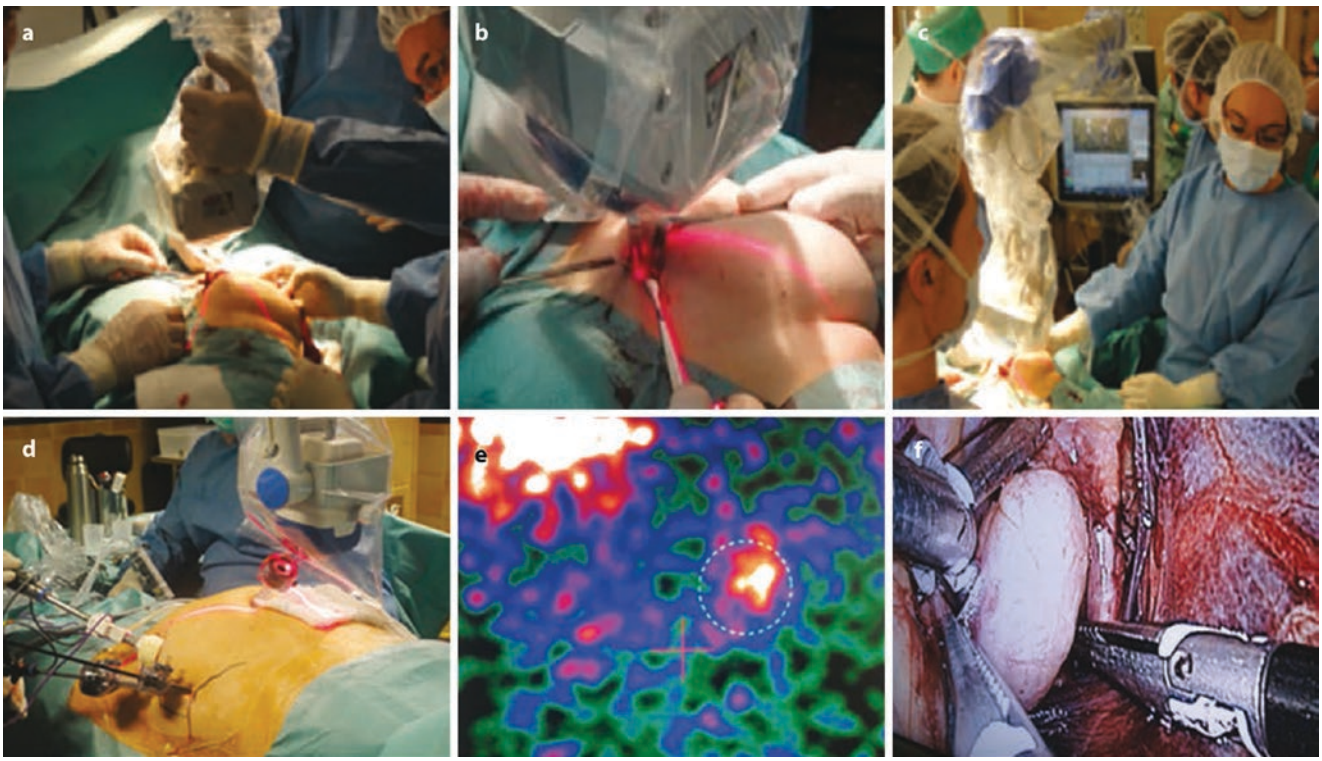

Fig. 7.14 Portable gamma camera intraoperative approach. The device is placed over the interest area in the most convenient way (**a**). A red cross shows the central position of image on the gamma camera's screen (**b**). This feature allows a better comprehension and awareness about the potential SLNs on the surgical field (**c**). Lower row: Laparoscopic approach. The portable gamma camera is positioned over abdominal wall to continuously assess the tracer uptake (**d**). Usual uptake in a SLN close to the common iliac vein (green circle; **e**). This node was clearly located in that area and subsequently removed (**f**)

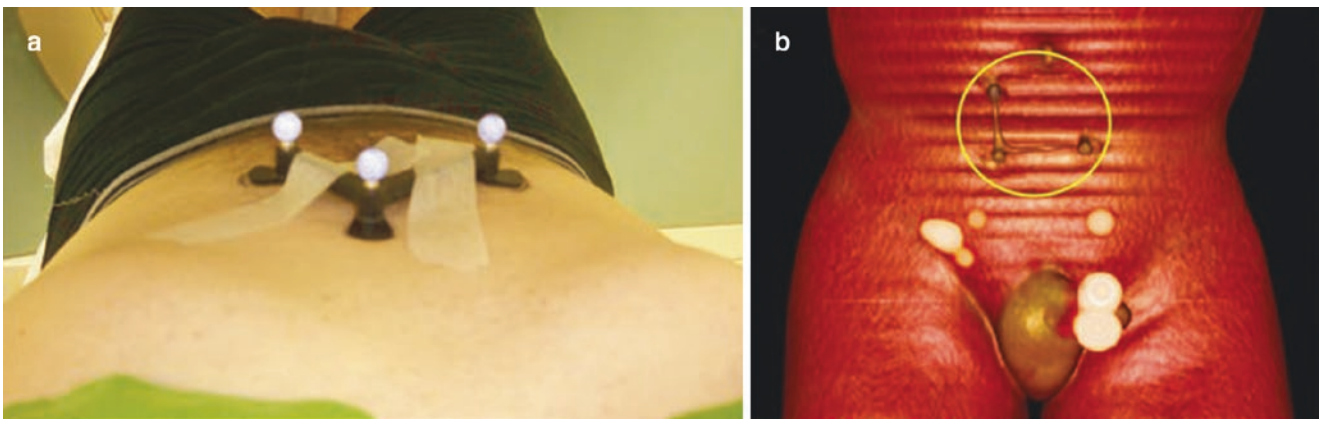

Fig. 7.15 (**a**) Positioning of the tracking device positioned on the patient's body for radioguided SLNB in a patient with penile cancer (same patient as in Fig. 7.8). (**b**) 3D volume-rendering SPECT/CT, showing the pattern of lymphatic drainage in a patient with penile cancer (approximate position of the tracking device on the patient's body is also indicated in the yellow circle). (**c**) Tracking device attached to a gamma probe in order to generate freehand SPECT data. (**d**) By integrating preoperative SPECT/CT data it is possible to overlay the generated 3D image to the patient's body with simultaneous display of the SLNs on the right side of the pelvis

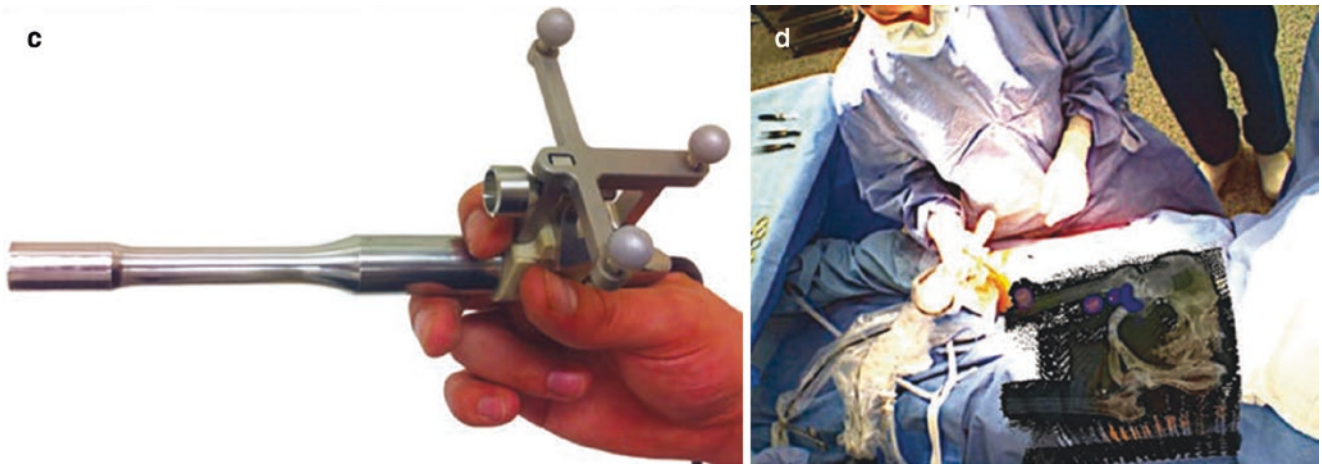

Fig. 7.15 (continued)

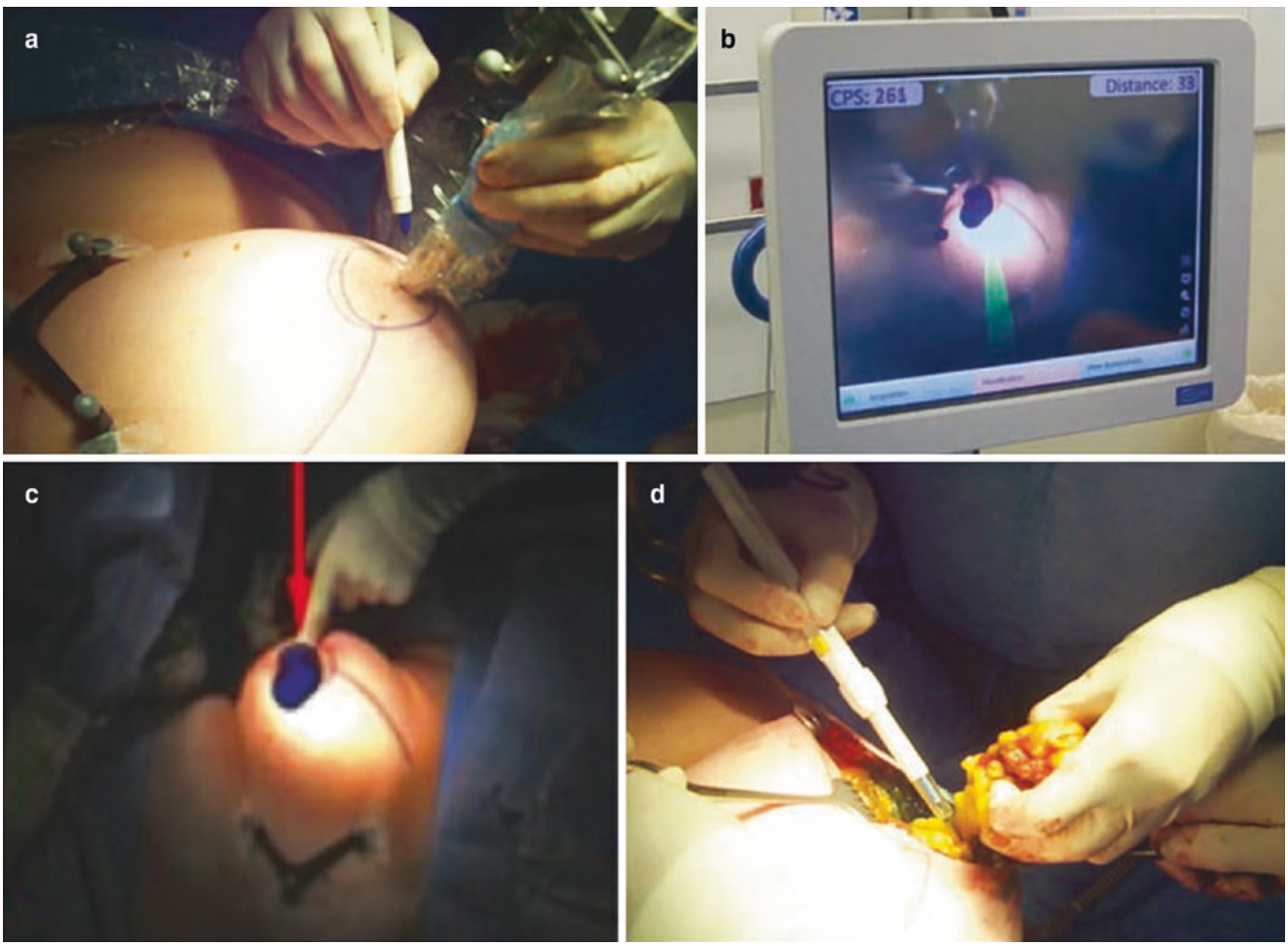

Fig. 7.16 Free-hand SPECT system used for radioguided occult lesion localization (ROLL) in a patient with non-palpable breast cancer. (**a**) Surgical approach for ROLL; the tracking device positioned on the patient's body is visible on the left. (**b**, **c**) Overlay of freehand SPECT 3D images on the video displays, with the red arrow in panel C indicating the site of the tumor. (**d**) Completion of lumpectomy guided by the freehand SPECT-based system

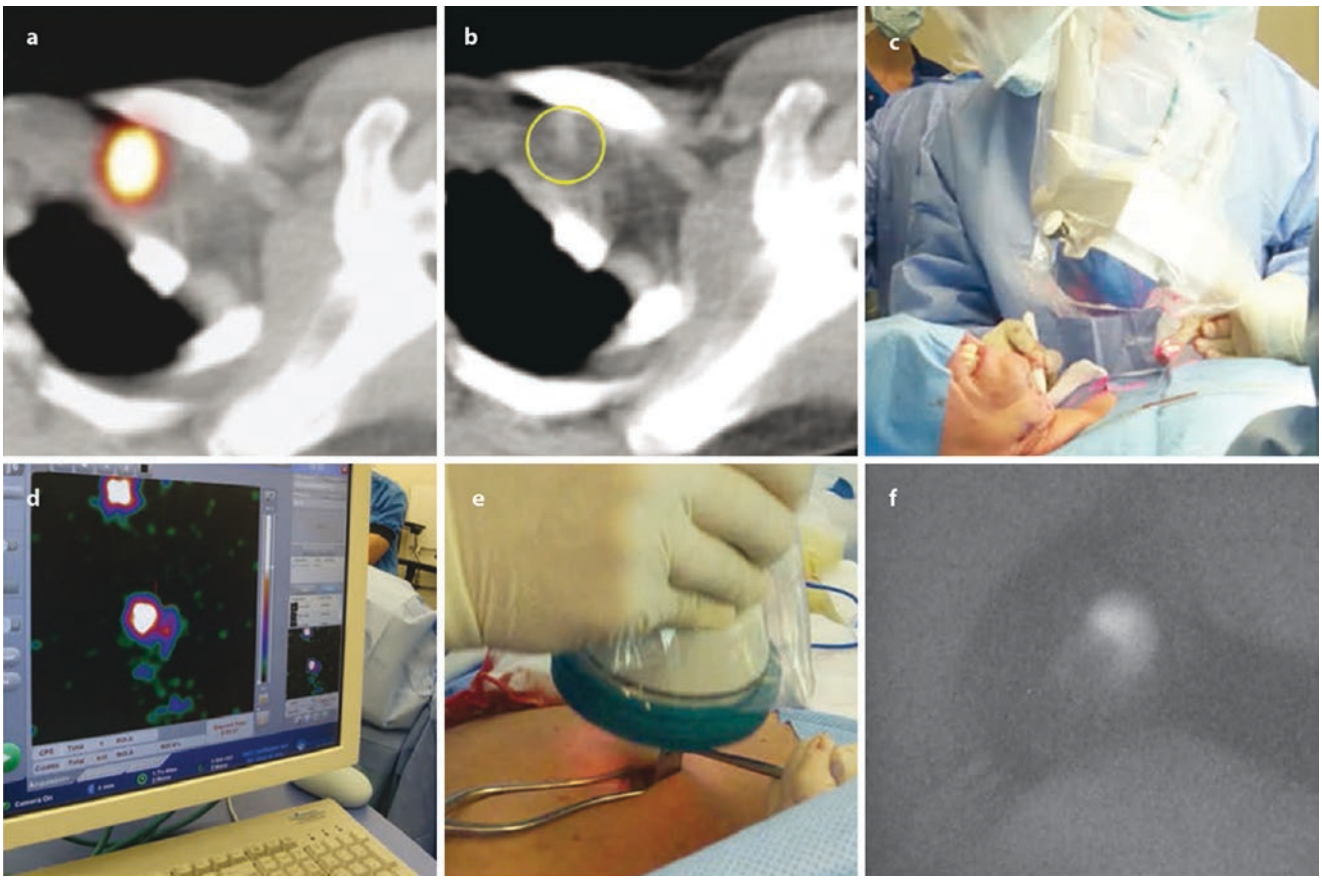

Fig. 7.17 (**a**) Fused axial SPECT/CT section showing a radioactive SLN in the left cervical area. (**b**) This focus of radioactive accumulation corresponds to a solitary lymph node seen in the CT section (circle). (**c**) The use of a portable gamma camera permits the surgeon to select the site for incision, and (**d**) also to monitor the procedure with intraoperative imaging guidance. The recent introduction of bimodal tracers for simultaneous radioguided (**e**) and fluorescent (**f**) detection is leading to the additional use of a fluorescence camera to better distinguish the SLN in anatomically complex areas

References

1. NCCN clinical practice guidelines in oncology (NCCN guidelines®) breast cancer, version 3.2019. https://www.nccn.org/professionals/physician_gls/pdf/breast.pdf.
2. NCCN clinical practice guidelines in oncology (NCCN guidelines®) cutaneous melanoma, version 2.2019. https://www.nccn.org/professionals/physician_gls/pdf/cutaneous_melanoma.pdf.
3. Giuliano AE, Hunt KK, Ballman KV, et al. Axillary dissection vs no axillary dissection in women with invasive breast cancer and sentinel node metastasis: a randomized clinical trial. JAMA. 2011;305:569–75.
4. Giammarile F, Vidal-Sicart S, Orsini F, et al. In: Volterrani D, Erba PA, Carrió I, Strauss HW, Mariani G, editors. Nuclear medicine textbook—methodology and clinical applications. Basel: Springer Nature; 2019. p. 351–90.
5. Galimberti V, Cole BF, Viale G, et al. Axillary dissection versus no axillary dissection in patients with breast cancer and sentinel-node micrometastases (IBCSG 23-01): 10-year follow-up of a randomised, controlled phase 3 trial. Lancet Oncol. 2018;19:1385–93.
6. Giuliano AE, Han SH. Local and regional control in breast cancer: role of sentinel node biopsy. Adv Surg. 2011;45:101–16.
7. Orsini F, Puta E, Mariani G. Single-photon emitting radiopharmaceuticals. In: Volterrani D, Erba PA, Carrió I, Strauss HW, Mariani G, editors. Nuclear medicine texbook—methodology and clinical applications. Basel: Springer Nature; 2019. p. 21–56.
8. Vidal-Sicart S, Vera D, Valdés Olmos RA. Next generation of radiotracers for sentinel lymph node biopsy: what is still necessary to establish new imaging paradigms? Rev Esp Med Nucl Imagen Mol. 2018;37:373–9.
9. KleinJan GH, van Werkhoven E, van den Berg NS, et al. The best of both worlds: a hybrid approach for optimal pre- and intraoperative identification of sentinel lymph nodes. Eur J Nucl Med Mol Imaging. 2018;45:1915–25.
10. Brouwer OR, Buckle T, Vermeeren L, et al. Comparing the hybrid fluorescent-radioactive tracer indocyanine green-^{99m}Tc-nanocolloid with ^{99m}Tc-nanocolloid for sentinel node identification: a validation study using lymphoscintigraphy and SPECT/CT. J Nucl Med. 2012;53:1034–40.

11. Goyal A, Newcombe RG, Mansel RE, et al. Role of routine preoperative lymphoscintigraphy in sentinel node biopsy for breast cancer. Eur J Cancer. 2005;41:238–43.
12. Even-Sapir E, Lerman H, Lievshitz G, et al. Lymphoscintigraphy for sentinel node mapping using a hybrid SPECT/CT system. J Nucl Med. 2003;44:1413–20.
13. Lerman H, Metser U, Lievshitz G, et al. Lymphoscintigraphic sentinel node identification in patients with breast cancer: the role of SPECT/CT. Eur J Nucl Med Mol Imaging. 2006;33:329–37.
14. Lerman H, Lievshitz G, Zak O, et al. Improved sentinel node identification by SPECT/CT in overweight patients with breast cancer. J Nucl Med. 2007;48:201–6.
15. Zanzonico P, Heller S. The intraoperative gamma probe: basic principles and choices available. Semin Nucl Med. 2000;30:33–48.
16. Mathelin CE, Guyonnet JL. Scintillation crystal or semiconductor gamma-probes: an open debate. J Nucl Med. 2006;47:373.
17. Meller B, Sommer K, Gerl J, et al. High energy probe for detecting lymph node metastases with ^{18}F-FDG in patients with head and neck cancer. Nuklearmedizin. 2006;45:153–9.
18. Curtet C, Carlier T, Mirallié E, et al. Prospective comparison of two gamma probes for intraoperative detection of ^{18}F-FDG: in vitro assessment and clinical evaluation in differentiated thyroid cancer patients with iodine-negative recurrence. Eur J Nucl Med Mol Imaging. 2007;34:1556–62.
19. Schneebaum S, Essner R, Even-Sapir E. Positron-sensitive probes. In: Mariani G, Giuliano AE, Strauss HW, editors. Radioguided surgery—a comprehensive team approach. New York: Springer; 2008. p. 23–8.
20. Valdés Olmos RA, Vidal-Sicart S, Manca G, et al. Advances in radioguided surgery. Q J Nucl Med Mol Imaging. 2017;61:247–70.
21. Rauscher I, Horn T, Gschwend JE, et al. Novel technology of molecular radio-guidance for lymph node dissection in recurrent prostate cancer by PSMA-ligands. World J Urol. 2018;36:603–8.
22. Van Oosterom MN, Rietbergen DDD, Welling MM, et al. Recent advances in nuclear and hybrid detection modalities for image-guided surgery. Expert Rev Med Devices. 2019;16:711–34.
23. Vermeeren L, van der Ploeg IM, Valdés Olmos RA, et al. SPECT/CT for preoperative sentinel node localization. J Surg Oncol. 2010;101:184–90.
24. Israel O, Pellet O, Biassoni L, et al. Two decades of SPECT/CT—the coming of age of a technology. An updated review of the literature evidence. Eur J Nucl Med Mol Imaging. 2019;46:1990–2012.
25. Kobayashi K, Ramirez PT, Kim EE, et al. Sentinel node mapping in vulvovaginal melanoma using SPECT/CT lymphoscintigraphy. Clin Nucl Med. 2009;34:859–61.
26. Leijte JA, van der Ploeg IM, Valdés Olmos RA, et al. Visualization of tumor blockage and rerouting of lymphatic drainage in penile cancer patients by use of SPECT/CT. J Nucl Med. 2009;50:364–7.
27. van der Ploeg IM, Valdés Olmos RA, Kroon BB, et al. The yield of SPECT/CT for anatomical lymphatic mapping in patients with melanoma. Ann Surg Oncol. 2009;16:1537–42.
28. Vermeeren L, Valdés Olmos RA, Meinhardt W, et al. Value of SPECT/CT for detection and anatomic localization of sentinel lymph nodes before laparoscopic sentinel node lymphadenectomy in prostate carcinoma. J Nucl Med. 2009;50:865–70.
29. Pandit-Taskar N, Gemignani ML, Lyall A, et al. Single photon emission computed tomography SPECT-CT improves sentinel node detection and localization in cervical and uterine malignancy. Gynecol Oncol. 2010;117:59–64.
30. Vermeeren L, Meinhardt W, Valdés Olmos RA. Prostatic lymphatic drainage with sentinel nodes at the ventral abdominal wall visualized with SPECT/CT: a case series. Clin Nucl Med. 2010;35:71–3.
31. Vermeeren L, Valdés Olmos RA, Klop WM, et al. SPECT/CT for sentinel lymph node mapping in head and neck melanoma. Head Neck. 2011;33:1–6.
32. Giammarile F, Alazraki N, Aarsvold JN, et al. The EANM and SNMMI practice guideline for lymphoscintigraphy and sentinel node localization in breast cancer. Eur J Nucl Med Mol Imaging. 2013;40:1932–47.
33. Cox CE, Cox JM, Mariani G, et al. Sentinel lymph node biopsy in patients with breast cancer. In: Mariani G, Giuliano AE, Strauss HW, editors. Radioguided surgery—a comprehensive team approach. New York: Springer; 2008. p. 87–97.
34. Estourgie SH, Nieweg OE, Valdés Olmos RA, et al. Eight false negative sentinel lymph node procedures in breast cancer: what went wrong? Eur J Surg Oncol. 2003;29:336–40.
35. Serrano Vicente J, Infante de la Torre JR, Domínguez Grande ML, et al. Optimization of sentinel lymph node biopsy in breast cancer by intraoperative axillary palpation. Rev Esp Med Nucl. 2010;29:8–11.
36. Varghese P, Abdel-Rahman AT, Akberali S, et al. Methylene blue dye—a safe and effective alternative for sentinel lymph node localization. Breast J. 2008;14:61–7.
37. Rodier JF, Velten M, Wilt M, et al. Prospective multicentric randomized study comparing periareolar and peritumoral injection of radiotracer and blue dye for the detection of sentinel lymph node in breast sparing procedures: FRANSENODE trial. J Clin Oncol. 2007;25:3664–9.
38. Valdés Olmos RA, Vidal-Sicart S, Nieweg OE. SPECT-CT and real-time intraoperative imaging: new tools for sentinel node localization and radioguided surgery? Eur J Nucl Med Mol Imaging. 2009;36:1–5.
39. Vermeeren L, Valdés Olmos RA, Meinhardt W, et al. Intraoperative radioguidance with a portable gamma camera: a novel technique for laparoscopic sentinel node localisation in urological malignancies. Eur J Nucl Med Mol Imaging. 2009;36:1029–36.
40. Hoffman EJ, Tornai MP, Janecek M, et al. Intra-operative probes and imaging probes. Eur J Nucl Med. 1999;26:913–35.
41. Mathelin C, Salvador S, Huss D, et al. Precise localization of sentinel lymph nodes and estimation of their depth using a prototype intraoperative mini gamma-camera in patients with breast cancer. J Nucl Med. 2007;48:623–9.
42. Scopinaro F, Tofani A, di Santo G, et al. High-resolution, hand-held camera for sentinel-node detection. Cancer Biother Radiopharm. 2008;23:43–52.
43. Zaknun JJ, Giammarile F, Valdés Olmos RA, et al. Changing paradigms in radioguided surgery and intraoperative imaging: the GOSTT concept. Eur J Nucl Med Mol Imaging. 2012;39:1–3.
44. Vermeeren L, Klop WM, van den Brekel MW, et al. Sentinel node detection in head and neck malignancies: innovations in radioguided surgery. J Oncol. 2009;2009:681746.
45. Duch J. Portable gamma cameras: the real value of an additional view in the operating theatre. Eur J Nucl Med Mol Imaging. 2011;38:633–5.
46. Vidal-Sicart S, Paredes P, Zanón G, et al. Added value of intraoperative real-time imaging in searches for difficult-to-locate sentinel nodes. J Nucl Med. 2010;51:1219–25.
47. Leong SP, Wu M, Lu Y, et al. Intraoperative imaging with a portable gamma camera may reduce the false-negative rate for melanoma sentinel lymph node surgery. Ann Surg Oncol. 2018;25:3326–33.
48. Wendler T, Herrmann K, Schnelzer A, et al. First demonstration of 3-D lymphatic mapping in breast cancer using freehand SPECT. Eur J Nucl Med Mol Imaging. 2010;37:1452–61.
49. Rieger A, Saeckl J, Belloni B, et al. First experiences with navigated radio-guided surgery using freehand SPECT. Case Rep Oncol. 2011;4:420–5.

50. van der Poel HG, Buckle T, Brouwer OR, et al. Intraoperative laparoscopic fluorescence guidance to the sentinel lymph node in prostate cancer patients: clinical proof of concept of an integrated functional imaging approach using a multimodal tracer. Eur Urol. 2011;60:826–33.
51. Keereweer S, Kerrebijn JD, van Driel PB, et al. Optical image-guided surgery—where do we stand? Mol Imaging Biol. 2011;13:199–207.
52. Polom K, Murawa D, Rho YS, et al. Current trends and emerging future of indocyanine green usage in surgery and oncology: a literature review. Cancer. 2011;117:4812–22.
53. Namazov A, Volchok V, Liboff A, et al. Sentinel nodes detection with near-infrared imaging in gynecological cancer patients: ushering in an era of precision medicine. Isr Med Assoc J. 2019;21:390–3.